Biophysical characterization of interactions between the core binding factor α and β subunits and DNA

Yen-Yee Tang[a], Barbara E. Crute[a], John J. Kelley III[b], Xuemei Huang[b], Jiangli Yan[b], Jianxia Shi[b], Kari L. Hartman[c], Thomas M. Laue[c], Nancy A. Speck[a], John H. Bushweller[b,*]

[a]*Department of Biochemistry, Dartmouth Medical School, Hanover, NH 03755, USA*
[b]*Department of Molecular Physiology and Biological Physics, University of Virginia, Charlottesville, VA 22906-0011, USA*
[c]*Department of Biochemistry, University of New Hampshire, Durham, NH 03824, USA*

Received 24 January 2000

Edited by Claude Klee

Abstract Core binding factors (CBFs) play key roles in several developmental pathways and in human disease. CBFs consist of a DNA binding CBFα subunit and a non-DNA binding CBFβ subunit that increases the affinity of CBFα for DNA. We performed sedimentation equilibrium analyses to unequivocally establish the stoichiometry of the CBFα:β:DNA complex. Dissociation constants for all four equilibria involving the CBFα Runt domain, CBFβ, and DNA were defined. Conformational changes associated with interactions between CBFα, CBFβ, and DNA were monitored by nuclear magnetic resonance and circular dichroism spectroscopy. The data suggest that CBFβ 'locks in' a high affinity DNA binding conformation of the CBFα Runt domain.

Key words: Core binding factor; AML1; Runx1; Core binding factor β; Transcription; Biophysical

1. Introduction

Core binding factors (CBFs, also known as PEBP2) are heterodimeric transcription factors consisting of a DNA binding subunit (CBFα) and a non-DNA binding CBFβ subunit [1–4]. CBFα subunits are encoded by three genes in mammals, *Runx1*, *Runx2*, and *Runx3* (formerly called *Cbfa2*, *Cbfa1*, and *Cbfa3*, also known as *Pebpa2b*, *Pebpa2a*, and *Pebpa2c*, or *AML1*, *AML3*, and *AML2*, respectively) [3,5–8]. CBFβ is encoded by one gene, *Cbfb* (or *Pebpb2*) [2,4]. Homozygous disruption of either the *Runx1* or *Cbfb* gene results in identical defects, including embryonic lethality from extensive hemorrhaging in the central nervous system and a severe block at the fetal liver stage of hematopoiesis [9–13]. The *Runx2* gene is required for bone formation [14,15], while the in vivo function of *Runx3* is unknown. Mutations in the one copy of the *RUNX2 (CBFA1)* gene cause cleidocranial dysplasia, an inherited skeletal abnormality [16]. Haploinsufficiency of *RUNX1* causes a familial platelet disorder with predisposition for acute myeloid leukemia [17]. A large proportion of acute leukemias and a smaller number of therapy-related leukemias are associated with chromosomal translocations involving the *RUNX1* and *CBFB* genes [18], or point mutations in one or both copies of the *RUNX1* gene [17,19].

The Runt domain of the CBFα subunits both binds DNA and heterodimerizes with the CBFβ subunit [3,20]. The Runt domain alone can bind DNA in vitro, but its affinity for DNA increases in the presence of CBFβ. CBFβ does not appear to establish contacts with additional phosphates or purine bases in the DNA [1,4], therefore it was proposed that CBFβ stabilizes a conformation of CBFα that is favorable for DNA binding [4,21]. Here we provide experimental support for this hypothesis.

2. Materials and methods

2.1. Protein and DNA preparation

The full length CBFβ(187) protein, the CBFβ heterodimerization domain [CBFβ(141)], and an amino acid 41–214 Runt domain fragment from Runx1 (AML1, hereafter referred to as CBFα) were expressed and purified as described previously [22–24]. Two complementary strands of a high affinity CBF binding site [25] were synthesized and purified via anion exchange chromatography (Midland Certified Reagent Company). Annealed double-stranded oligonucleotides were separated from single-stranded material by chromatography on Q-Sepharose. The final purified DNA was exchanged into the appropriate buffer by lyophilization and size exclusion chromatography on Sephadex G25.

2.2. Sedimentation equilibrium

Complexes of the Runx1 Runt domain (CBFα), CBFβ, and DNA were prepared by combining appropriate quantities of dialyzed protein and/or DNA to obtain final complex concentrations of 31 μM. High speed sedimentation equilibrium experiments [26] were conducted at 20°C in a Beckman XL-1 ultracentrifuge at rotor speeds of 20 000, 25 000, 30 000, and 40 000 rpm using interference detection. Three cell loading concentrations were examined (15–3.75 μM) in 20 mM potassium phosphate (pH 7.5), 25 mM KCl, 0.5 mM dithiothreitol (DTT). Data were fit using NONLIN [27]. The solvent density (1.002 g/ml), Runt domain monomer molecular weight (19 112 g/mol), formal charge (+8.5) and partial specific volume (0.7341 ml/g), as well as the CBFβ monomer molecular weight (22 103 g/mol), formal charge (−5) and partial specific volume (0.7161) were calculated using the program Sednterp [28]. The expected molecular weight (41 215 g/mol) and partial specific volume (0.7244) of the CBFα:β complex were calculated from these subunit values. For the 18 bp DNA, a composition (9 A, 9 T, 9 C and 9 G) molecular weight of 11 547 g/mol is calculated. Ordinarily, a partial specific volume of 0.54 ml/g is assumed for long duplex DNA in physiological solvents [29]. However, for a DNA oligonucleotide bound to a protein, the partial specific volume is difficult to estimate. Assuming 0.54 ml/g for the DNA, partial specific volumes of 0.6763 ml/g and 0.6939 ml/g were calculated for the CBFα:DNA and CBFα:β:DNA complexes respectively, and an additional uncertainty of 0.01 ml/g in the partial specific volumes was included when calculating molecular weights for these two complexes.

2.3. Dissociation constant measurements

The core site from the SL3-3 murine leukemia virus enhancer was used to measure binding of CBFα to DNA in the presence or absence

*Corresponding author. Fax: (1)-804-982 1616.
E-mail: jhb4v@virginia.edu

PII: S0014-5793(00)01312-0

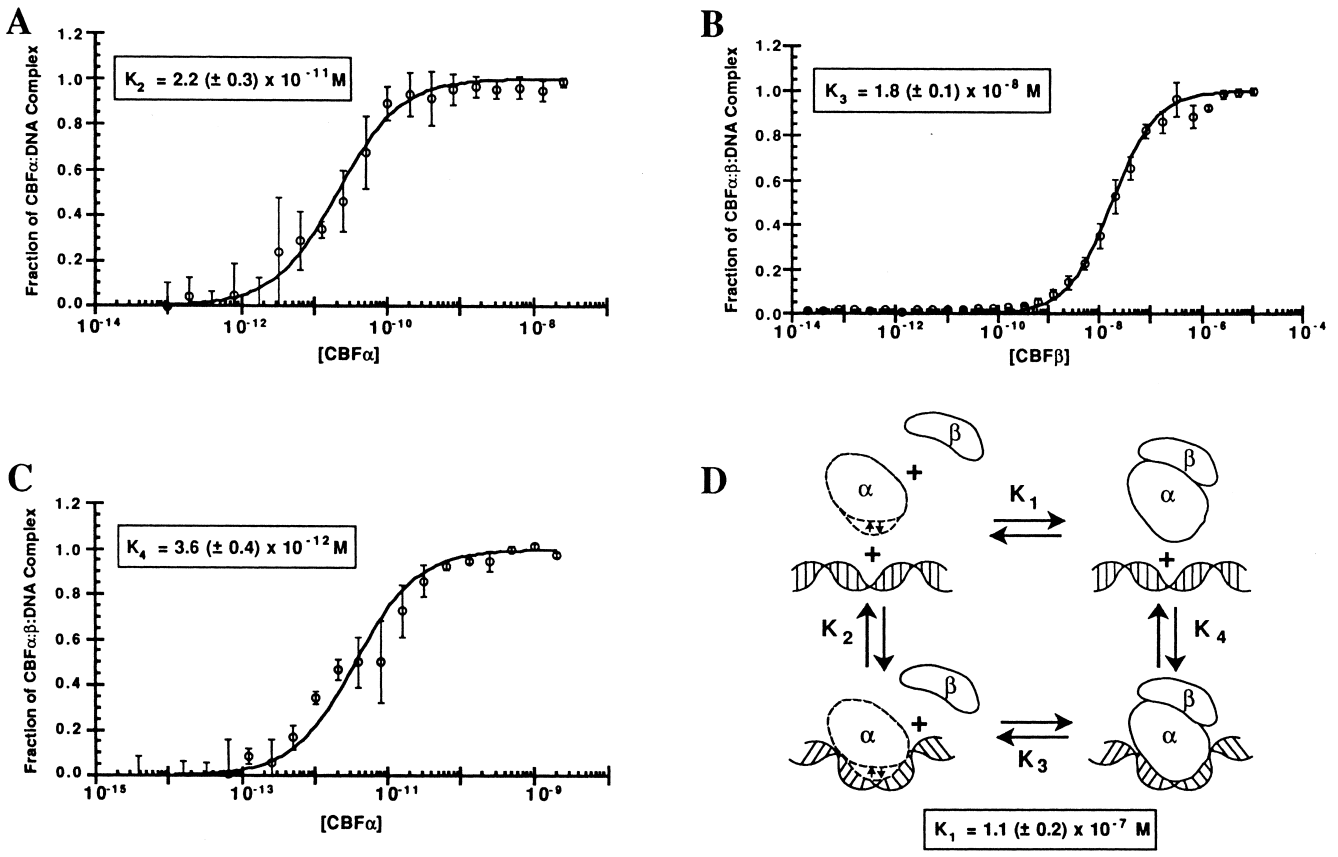

Fig. 1. Equilibrium DNA binding studies of CBFα, CBFβ, and DNA. Data are presented as the mean (+S.D.) of three independent experiments. A: Determination of K_2 describing binding of the CBFα Runt domain to DNA. B: Determination of K_3 describing the interaction of CBFβ with CBFα:DNA. C: Determination of K_4 describing the binding of CBFα:β to DNA. D: Schematic representation of the conformational changes occurring in CBFα, CBFβ, and DNA. The calculated (K_1) equilibrium dissociation constant is indicated.

of CBFβ(187). Equilibrium binding constants of CBFα for DNA, and CBFβ(187) for a CBFα:DNA complex were measured by electrophoretic mobility shift assay (EMSA), and analyzed as described previously [22,23]. The affinity of CBFα:β for DNA was determined by titrating CBFα onto a fixed amount of DNA (2×10^{-13} M) in the presence of 5 μM CBFβ(187).

2.4. Isothermal titration calorimetry

The equilibrium binding constant for the formation of a CBFα:β complex was determined by isothermal titration calorimetry (ITC). All measurements were carried out at 10°C on a MicroCalorimetry System MCS ITC (MicroCal Inc.). A solution of 47.5 μM CBFα was titrated with aliquots of 595 μM CBFβ(141)(A137S). Ligand dilution enthalpies were subtracted from the titration, and data were fitted to a one-site model using Origin (MicroCal Inc.).

2.5. Circular dichroism (CD) spectroscopy

CD experiments were performed at 20°C on a Jasco 715 spectrometer calibrated using 10-camphorsulfonic acid. The experiments were performed with a 1.0 nm band width, and data points taken every 0.5 nm with an 8 s averaging time. Measurements in the far UV (205–325 nm) of binary and ternary complexes were performed using a Hellma quartz mixing cuvette. A non-interacting CD spectrum was measured by averaging four scans. The mixing cell was then inverted several times, allowing samples from the two chambers to flow into the mixing cavity, and the complexed or interacting CD spectrum recorded also with four scans. The concentration of all protein and DNA components was 2.5 μM in 20 mM potassium phosphate (pH 7.5), 25 mM potassium chloride, and 0.5 mM DTT. The ellipticity values for the buffer were subtracted from the experimental values obtained for uncomplexed and complexed protein–DNA samples. No smoothing of the data was applied at any stage.

2.6. NMR spectroscopy

The ternary CBFα:β:DNA complex was prepared by adding unlabeled CBFβ(141) to a sample of 100% ^{2}H,^{13}C,^{15}N-labeled Runx1 Runt domain complexed to unlabeled DNA [24]. TROSY-based HNCA, HN(CA)CB, HNCO, and ^{15}N-edited NOESY spectra [30] were recorded under the conditions used for backbone assignment previously [24]. ^{15}N amino acid specifically labeled samples of the Runt domain [24] were also titrated with unlabeled CBFβ(141) and 2D TROSY spectra recorded to assist in the resonance assignments. All experiments were carried out on a 600 MHz Varian Innova spectrometer equipped with a Nalorac triple resonance gradient probe.

Table 1
Results of sedimentation equilibrium analyses of CBFα Runt domain complexes: global fits of data for a single ideal species model

Sample	M_z (g/mol)[a]	RMS[b]	Expected MW
CBFα:DNA	26 500 (25 400–27 740)	0.017	30 660
CBFα:β	41 003 (40 984–41 022)	0.015	41 220
CBFα:β:DNA	46 290 (43 760–49 000)	0.031	52 760

[a]z-average molecular weight calculated from NONLIN values, calculated assuming a partial specific volume of 0.54 ml/g for the DNA.
[b]Root mean square of the variance of fit.

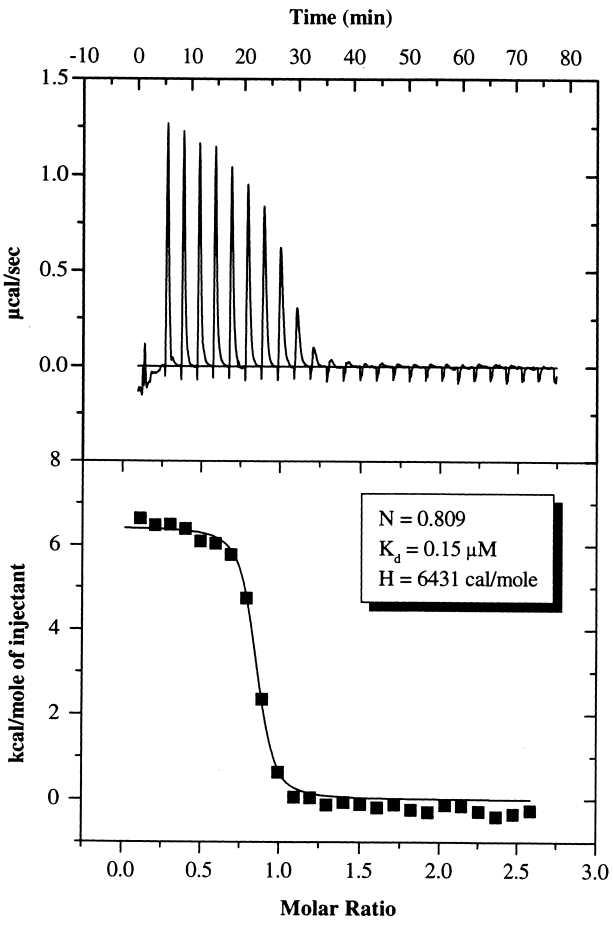

Fig. 2. Isothermal calorimetric titration of CBFα with CBFβ(141)(A137S). Top: Raw data from the addition of 10 µl aliquots of 595 µM CBFβ(141)(A137S) to 47.5 µM Runx1(41–214) (CBFα). Bottom: Results from the least squares fit to a one binding site model of the heat exchanged per mol of CBFβ(141)(A137S) versus the molar ratio of CBFβ(141)(A137S) to CBFα. Numerical values for the stoichiometry (N), equilibrium dissociation constant (K_1), and the molar change in enthalpy (H) are given in the box.
→

The resulting ^{15}N and NH assignments were compared to those obtained previously for the binary Runt domain–DNA complex [24].

A ternary complex containing 100% ^{2}H,^{13}C,^{15}N-labeled CBFβ(141) was prepared by addition of unlabeled CBFα:DNA complex to the labeled CBFβ(141). TROSY-based HNCA, HN(CA)CB, HNCO, and ^{15}N-edited NOESY spectra [30] were recorded as above to obtain complete backbone resonance assignments. Chemical shifts for uncomplexed CBFβ(141) were taken from Huang et al. [31].

3. Results and discussion

3.1. Stoichiometry

The stoichiometries of the CBFα:β, CBFα:DNA and CBFα:β:DNA complexes were established by sedimentation equilibrium (Table 1). All complexes sedimented as single ideal components with molecular weights consistent with 1:1 (CBFα:β and CBFα:DNA) or 1:1:1 (CBFα:β:DNA) complexes. The measured molecular weight of CBFα:β is within 0.6% of the predicted value. While the molecular weights calculated for the two protein–DNA complexes are consistent with the expected stoichiometries, the molecular weights are almost 15% lower than anticipated. These lower molecular weights are not a consequence of dissociation, since there is no systematic decrease in the molecular weights with decreasing concentration. Likewise, there is no systematic increase in molecular weight with decreasing concentration, indicating

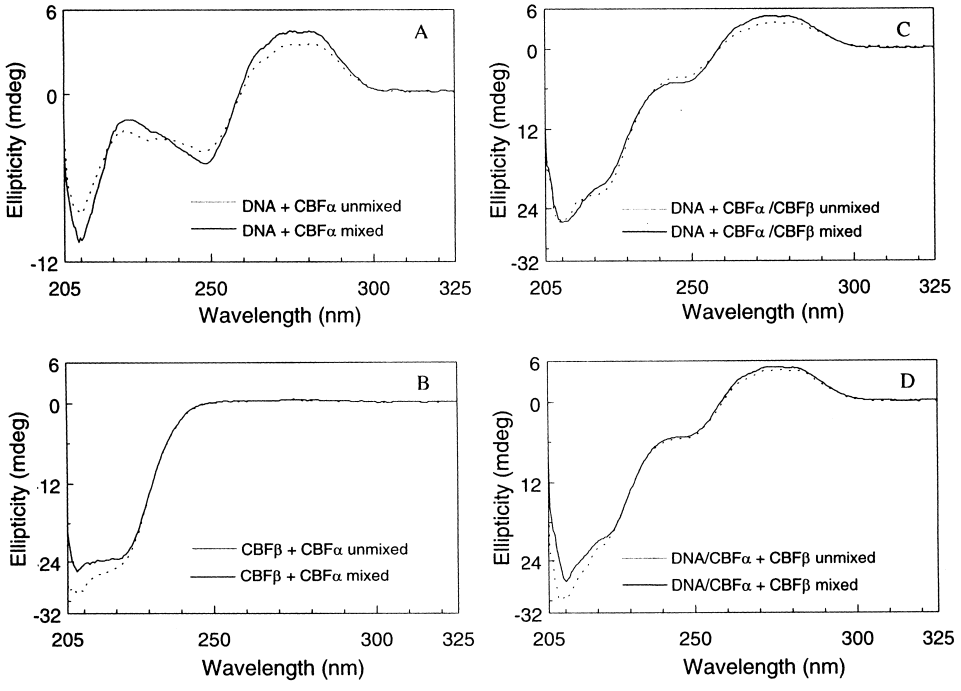

Fig. 3. Conformational changes in the CBF subunits and DNA monitored by far UV circular dichroism. In all cases dotted lines represent unmixed spectra, and solid lines represent mixed (complexed) spectra.

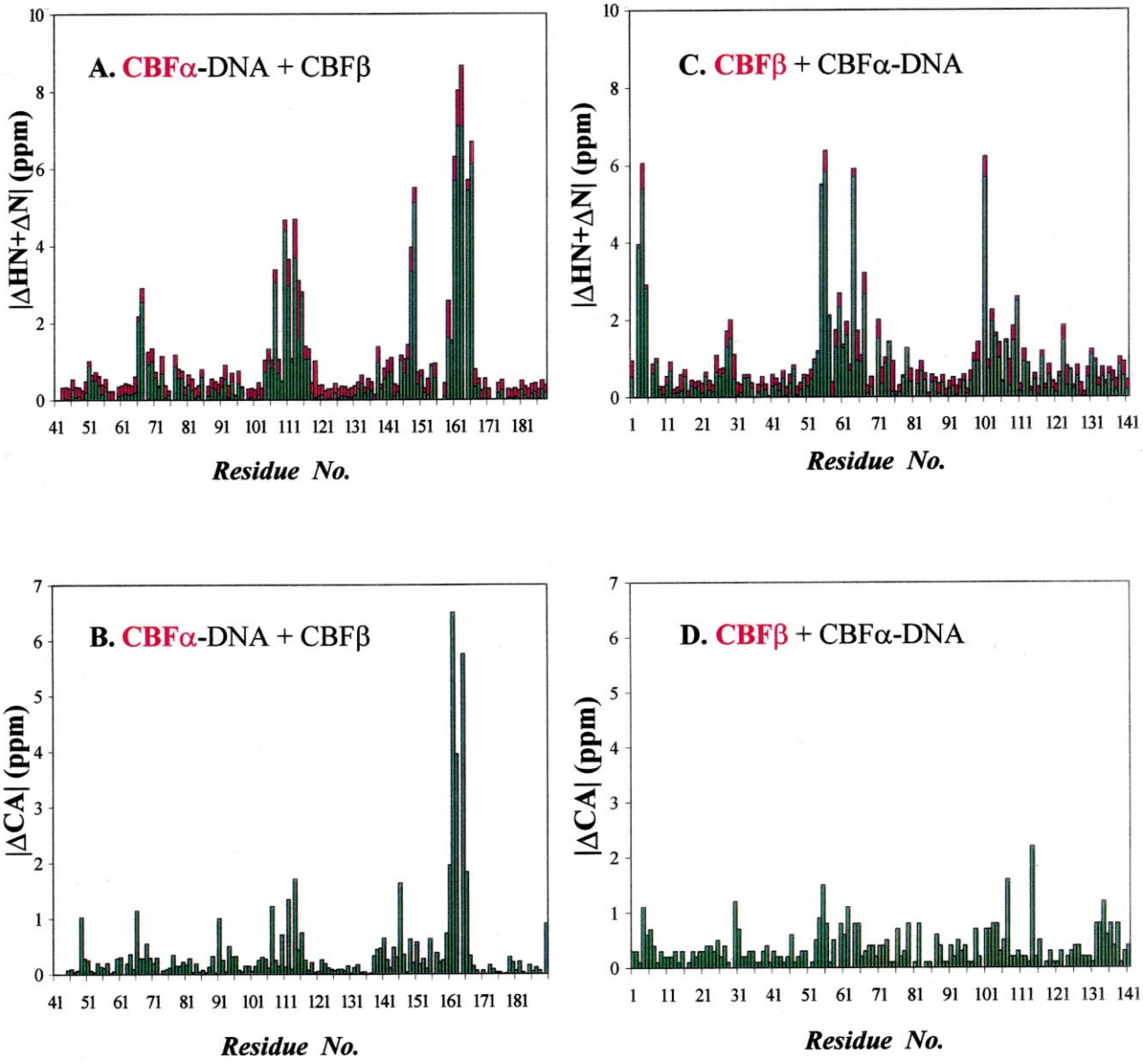

Fig. 4. NMR chemical shift perturbation mapping of the CBFα:β interaction. A: NH chemical shift changes in CBFα upon binding of CBFβ. The Runt domain is numbered relative to the AML1 protein [5]. ^{15}N shifts are in green and HN shifts are in red. B: Cα chemical shift changes in the Runx1 Runt domain (CBFα) upon binding of CBFβ. C: NH chemical shift changes in CBFβ upon binding of CBFα:DNA. ^{15}N shifts are in green and HN shifts are in red. D: Cα chemical shift changes in CBFβ upon binding of CBFα:DNA.

that the lower molecular weight is not a consequence of sample heterogeneity or thermodynamic non-ideality [26,27]. These observations suggest that the partial specific volume of the complexes is about 0.04 ml/g larger than calculated assuming a partial specific volume of 0.54 ml/g for the DNA. An increased partial specific volume for the DNA would be expected if complex formation reduces its net charge and alters the counterion binding significantly.

3.2. Measurement of dissociation constants

We carried out a detailed analysis of the binding constants describing the interactions between CBFα, CBFβ, and DNA by EMSA (Fig. 1). K_2 is the dissociation constant for CBFα binding to DNA (Fig. 1A). K_3 describes the binding of CBFβ to the CBFα:DNA complex (Fig. 1B). K_4 represents binding of the CBFα:β heterodimer to DNA (Fig. 1C). The measured dissociation constants allow us to calculate the value of K_1 describing the interaction between CBFα and CBFβ off DNA from the equation $K_2K_3 = K_1K_4$ (Fig. 1D). Comparison of the dissociation constants K_2 and K_4 and their errors shows that CBFβ causes a statistically significant six-fold enhancement in DNA binding by the CBFα Runt domain. The observed change in the K_d values corresponds to a $\Delta\Delta G$ of 1 kcal/mol associated with the binding of CBFα to DNA in the absence and presence of CBFβ.

We also measured K_1 directly by ITC to confirm the K_1 value calculated from EMSAs (Fig. 2). Attempts to obtain calorimetric data with CBFβ(141) yielded very small enthalpies and therefore poor quality data. In contrast, an A137→S mutant of CBFβ(141) yielded larger enthalpies and correspondingly better data. NMR data collected on CBFβ(141)(A137S) showed only minor perturbations relative

to CBFβ(141) which were isolated to the immediate vicinity of the mutation (not shown), thus the mutant protein retains the same fold as CBFβ(141). In addition, the C-terminal region of the last helix in CBFβ(141) where A137 is located is not involved in contacts with CBFα [31]. The value of K_1 obtained from calorimetry using CBFβ(141)(A137S) was 0.15 μM, in excellent agreement with the 0.11 μM value obtained indirectly from the EMSA measurements for the full length CBFβ.

3.3. CD spectroscopy

We employed a two-chambered mixing cell to record unmixed and mixed CD spectra associated with all the equilibria illustrated in Fig. 1. In Fig. 3A, the 'unmixed' spectrum represents the combined spectra of the isolated CBFα Runt domain and DNA in solution, while the 'mixed' spectrum corresponds to that of the CBFα:DNA complex. An increase in ellipticity at 275 nm and the very slight decrease at 250 nm suggest the DNA conformation changes upon CBFα binding. The changes observed at 275 nm are indicative of helix unwinding, in agreement with other results showing DNA is bent upon CBFα binding [32]. Unambiguous assignment of changes in the Runt domain conformation is not possible due to spectral overlap of protein and DNA in the 205–225 nm region.

Mixing experiments with CBFα and CBFβ document a substantial change in the 205–225 nm region of the spectrum (Fig. 3B), indicating that a significant conformational change occurs in one or both proteins upon heterodimerization. Binding of the preformed CBFα:β complex to DNA is accompanied by changes in the DNA region of the spectrum (230–275 nm) (Fig. 3C), closely resembling those induced by CBFα alone (Fig. 3A). Finally, when the pre-formed CBFα:DNA complex is mixed with CBFβ (Fig. 3D) there is a substantial change in the 205–225 nm region of the spectrum resembling that seen upon heterodimerization in solution (Fig. 3B), whereas the change in the DNA region of the spectrum (230–275 nm) is minor. In summary, the CD data indicate that heterodimerization of CBFα and CBFβ either in solution or on the DNA is accompanied by significant conformational changes in one or both proteins. CBFα by itself induces a conformational change in the DNA that is not significantly influenced by addition of the CBFβ subunit.

3.4. NMR spectroscopy

We added CBFβ(141) to ^{2}H,^{13}C,^{15}N-labeled Runt domain bound to unlabeled DNA, and assigned the backbone chemical shifts for the Runt domain. Comparison with the backbone chemical shifts of the Runt domain:DNA complex [24] provides a map of the CBFβ binding site (Fig. 4A). Substantial NH chemical shift perturbations (>2.0 ppm) in the Runt domain upon CBFβ binding were identified for 17 residues: 66, 67, 107, 110, 111, 113–115, 148, 149, 159–163, 165–166. Residue 164 was not assigned in the Runt domain:DNA complex [24], so no comparison data are available for this residue. Fig. 5 displays these residues on a ribbon representation of the Runt domain structure [24]. The highly perturbed residues map to one face of the protein, and clearly identify the surface utilized on the Runt domain for CBFβ binding. The general location of the CBFβ binding site is in agreement with another chemical shift perturbation study of this system [21], however the magnitude and locations of the observed changes differ. The dramatic changes observed between residues 159 and 166 were not reported previously because not all residues in this region were assigned [21]. Assignments for residues in this region and in the neighboring β-strand of the protein proved difficult to obtain because of apparent exchange broadening that degraded the quality of the triple resonance data. The quality of the triple resonance data in this region of the Runt domain in the ternary complex with CBFβ and DNA is substantially improved, and the exchange broadening seen in the binary Runt domain:DNA complex is apparently quenched (data not shown). This behavior is consistent with a model in which the Runt domain exchanges between two or more conformations in this region of the protein. Upon CBFβ binding, one conformation becomes locked in.

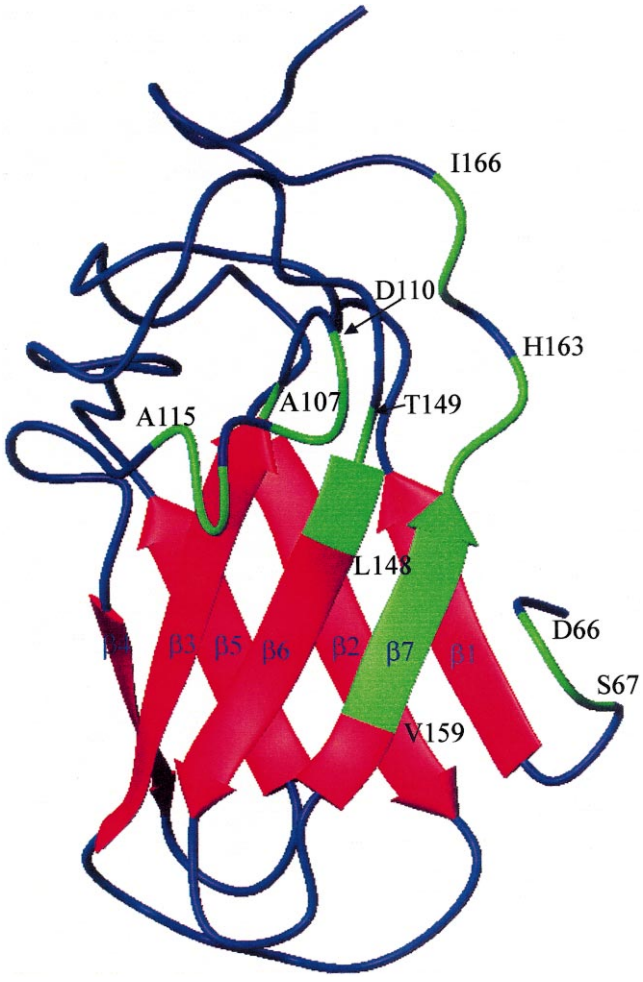

Fig. 5. Map of observed chemical shift changes from Fig. 4A on a ribbon diagram of the Runt domain. The β-strand regions are colored red. Loop regions, all of which have been implicated in close contacts with the DNA, are colored blue. Residues showing large perturbations upon CBFβ binding as described in the text are colored green.

Cα chemical shifts are relatively insensitive to contact-induced shifts, but are very sensitive indicators of the backbone dihedral angles [33], and thus provide a clear indicator of changes in backbone conformation, i.e. conformational changes. Fig. 4B shows the changes in the Cα chemical shifts in the Runt domain upon CBFβ binding. For comparison, the same data for CBFβ are given in Fig. 4D. The Cα chemical shift changes in the 159–166 region of the Runt domain are

significantly more dramatic than Cα chemical shift changes seen in CBFβ or in any other region of the Runt domain structure. The substantial nature of these changes strongly indicates that there is a conformational change in the Runt domain in this region upon CBFβ binding. As we have identified protein–DNA NOEs for residues just C-terminal to this region as well as in spatially proximal loops [24], perturbations here are very likely to alter the protein–DNA interface, and provide a rationale for the ability of CBFβ to increase the affinity of CBFα for DNA.

3.5. Conclusions

We have presented evidence from a variety of biophysical methods that CBFβ induces a localized conformational change in the CBFα (Runx1) Runt domain that increases the affinity of the Runt domain for DNA. The proximity of this site to residues known to be in contact with the DNA is consistent with this conformational change altering the protein–DNA interface in some manner. Definitive proof of this conformational change awaits detailed structural studies of these complexes, however the data presented strongly support such a model.

Acknowledgements: J.H.B. is supported by grants from the United States Public Health Service K02 AI01481, R29 AI39536, and R01 AI42097 from the Institute for Allergy and Infectious Disease. N.A.S. is supported by grants from United States Public Health Service R01CA 58343 and R01 CA75611. T.M.L. is supported by grants from the National Science Foundation BIR 9314040 and 9876582. Y.Y.T. is supported by T32 AI 07363 from the NIH/AID.

References

[1] Kamachi, Y., Ogawa, E., Asano, M., Ishida, S., Murakami, Y., Satake, M., Ito, Y. and Shigesada, K. (1990) J. Virol. 64, 4808–4819.
[2] Ogawa, E., Inuzuka, M., Maruyama, M., Satake, M., Naito-Fujimoto, M., Ito, Y. and Shigesada, K. (1993) Virology 194, 314–331.
[3] Ogawa, E., Maruyama, M., Kagoshima, H., Inuzuka, M., Lu, J., Satake, M., Shigesada, K. and Ito, Y. (1993) Proc. Natl. Acad. Sci. USA 90, 6859–6863.
[4] Wang, S., Wang, Q., Crute, B.E., Melnikova, I.N., Keller, S.R. and Speck, N.A. (1993) Mol. Cell. Biol. 13, 3324–3339.
[5] Miyoshi, H., Shimizu, K., Kozu, T., Maseki, N., Kaneko, Y. and Ohki, M. (1991) Proc. Natl. Acad. Sci. USA 88, 10431–10434.
[6] Ogawa, M. et al. (1993) Development 117, 1089–1098.
[7] Bae, S.C. et al. (1993) Oncogene 8, 809–814.
[8] Levanon, D., Negreanu, V., Bernstein, Y., Bar-Am, I., Avivi, L. and Groner, Y. (1994) Genomics 23, 425–432.
[9] Okuda, T., van Deursen, J., Hiebert, S.W., Grosveld, G. and Downing, J.R. (1996) Cell 84, 321–330.
[10] Wang, Q., Stacy, T., Binder, M., Marín-Padilla, M., Sharpe, A.H. and Speck, N.A. (1996) Proc. Natl. Acad. Sci. USA 93, 3444–3449.
[11] Wang, Q. et al. (1996) Cell 87, 697–708.
[12] Sasaki, K. et al. (1996) Proc. Natl. Acad. Sci. USA 93, 12359–12363.
[13] Niki, M. et al. (1997) Proc. Natl. Acad. Sci. USA 94, 5697–5702.
[14] Komori, T. et al. (1997) Cell 89, 755–764.
[15] Otto, F. et al. (1997) Cell 89, 765–772.
[16] Mundlos, S. et al. (1997) Cell 89, 773–780.
[17] Song, W.-J. et al. (1999) Nature Genet. 23, 166–175.
[18] Rubnitz, J.E. and Look, A.T. (1998) Curr. Opin. Hematol. 5, 264–270.
[19] Osato, M. et al. (1999) Blood 93, 1817–1824.
[20] Kagoshima, H., Shigesada, K., Satake, M., Ito, Y., Miyoshi, H., Ohki, M., Pepling, M. and Gergen, J.P. (1993) Trends Genet. 9, 338–341.
[21] Nagata, T. et al. (1999) Nature Struct. Biol. 6, 615–619.
[22] Huang, X. et al. (1998) J. Biol. Chem. 273, 2480–2487.
[23] Crute, B.E., Lewis, A.F., Wu, Z., Bushweller, J.H. and Speck, N.A. (1996) J. Biol. Chem. 271, 26251–26260.
[24] Berardi, M., Sun, C., Zehr, M., Abildgaard, F., Peng, J., Speck, N.A. and Bushweller, J.H. (1999) Structure 7, 1247–1256.
[25] Wang, S. and Speck, N.A. (1992) Mol. Cell. Biol. 12, 89–102.
[26] Yphantis, D.A. (1964) Biochemistry 3, 297–317.
[27] Johnson, M.L., Correia, J.J., Yphantis, D.A. and Halvorson, H.R. (1981) Biophys. J. 36, 575–588.
[28] Laue, T.M., Shah, B.D., Ridgeway, T.M. and Pelletier, S.L. (1992) in: Analytical Ultracentrifugation in Biochemistry and Polymer Science (Harding, S.E., Rowe, A.J. and Horton, J.C., Eds.), pp. 90–125, Royal Society of Chemistry, London.
[29] Durchschlag, H. (1989) Colloid Polym. Sci. 267, 1139–1150.
[30] Yang, D. and Kay, L.E. (1999) J. Biomol. NMR 13, 3–10.
[31] Huang, X., Peng, J.W., Speck, N.A. and Bushweller, J.H. (1999) Nature Struct. Biol. 6, 624–627.
[32] Golling, G., Li, L.-H., Pepling, M., Stebbins, M. and Gergen, J.P. (1996) Mol. Cell. Biol. 16, 932–942.
[33] Spera, S. and Bax, A. (1991) J. Am. Chem. Soc. 113, 5490–5492.